

DTIC FILE COPY

GL-TR-90-0044

AD-A224 400

Thermal Imaging Assessment

S. C. Richtsmeier  
M. E. Gersh

Spectral Sciences, Inc.  
99 South Bedford Street, #7  
Burlington, MA 01803-5169

22 February 1990

Scientific Report No. 2

DTIC  
ELECTE  
JUL 31 1990  
S E D

APPROVED FOR PUBLIC RELEASE; DISTRIBUTION UNLIMITED

GEOPHYSICS LABORATORY  
AIR FORCE SYSTEMS COMMAND  
UNITED STATES AIR FORCE  
HANSCOM AIR FORCE BASE, MASSACHUSETTS 01731-5000

"This technical report has been reviewed and is approved for publication"

*Edmond Murad*

EDMOND MURAD  
Contract Manager

*E. Murad*

for CHARLES P. PIKE, Chief  
Spacecraft Interactions Branch

FOR THE COMMANDER

*Rita C. Sagalyn (DEPUTY DIR.)*  
RITA C. SAGALYN, Director  
Space Physics Division

This report has been reviewed by the ESD Public Affairs Office (PA) and is releasable to the National Technical Information Service (NTIS)

Qualified requestors may obtain additional copies from the Defense Technical Information Center. All others should apply to the National Technical Information Service.

If your address has changed, or if you wish to be removed from the mailing list, or if the addressee is no longer employed by your organization, please notify AFGL/DAA, Hanscom AFB, MA, 01731. This will assist us in maintaining a current mailing list.

Do not return copies of this report unless contractual obligations or notices on a specific document requires that it be returned.

REPORT DOCUMENTATION PAGE

1a REPORT SECURITY CLASSIFICATION UNCLASSIFIED		1b RESTRICTIVE MARKINGS N/A	
2a SECURITY CLASSIFICATION AUTHORITY N/A		3 DISTRIBUTION/AVAILABILITY OF REPORT Approved for public release; distribution unlimited	
2b DECLASSIFICATION/DOWNGRADING SCHEDULE N/A		4 PERFORMING ORGANIZATION REPORT NUMBER(S) SSI-TR-171	
5 MONITORING ORGANIZATION REPORT NUMBER(S) GI-TR-90-0044		6a NAME OF PERFORMING ORGANIZATION Spectral Sciences, Inc.	
6b OFFICE SYMBOL (If applicable) N/A		7a. NAME OF MONITORING ORGANIZATION Geophysics Laboratory	
6c. ADDRESS (City, State, and ZIP Code) 99 South Bedford Street, #7 Burlington, MA 01803-5169		7b. ADDRESS (City, State, and ZIP Code) Hanscom AFB, MA 01731-5000	
8a NAME OF FUNDING/SPONSORING ORGANIZATION Geophysics Laboratory		8b. OFFICE SYMBOL (If applicable) 0111	
9. PROCUREMENT INSTRUMENT IDENTIFICATION NUMBER F19687-88-C-0074		9c ADDRESS (City, State, and ZIP Code) Hanscom AFB, MA 01731	
10. SOURCE OF FUNDING NUMBERS		11 TITLE (Include Security Classification) Thermal Imaging Assessment	
PROGRAM ELEMENT NO. 62101F	PROJECT NO. 7601	TASK NO. 30	WORK UNIT ACCESSION NO. BB
12 PERSONAL AUTHOR(S) S. C. Richtsmeier and M. E. Gersh			
13a TYPE OF REPORT Interim No. 2	13b. TIME COVERED FROM 15JAN90 TO 15FEB90	14 DATE OF REPORT (Year, Month, Day) 22 February 1990	15. PAGE COUNT 26
16 SUPPLEMENTARY NOTES			
17 COSMIL CC		18. SUBJECT TERMS (Continue on reverse if necessary and identify by block number)	
FIELD	GROUP	SUB-GROUP	thermal image
19 ABSTRACT (Continue on reverse if necessary and identify by block number) <p>This report investigates the feasibility of using advanced focal plane arrays coupled with telescopes as thermal imaging systems for orbiting targets. The infrared signature of a target will depend on a host of intercoupled factors including (1) surface properties (temperature, emissivity, reflectivity), (2) illumination conditions (solar position, earth background temperature), (3) target orientation, location, and dynamics with respect to the observer, and (4) atmospheric conditions along the illumination and target-observer paths. The determination of absolute surface temperatures of an unknown target is certainly a difficult if not infeasible problem without detailed knowledge of all of these factors. Here, we address the somewhat simpler problem of calculating the change in detected signal observed as a function of relative surface temperature differences, or conversely, given a sensor and its inherent characteristics, we attempt to determine the minimum detectable temperature difference measurable for a target surface of known characteristics.</p>			
20 DISTRIBUTION/AVAILABILITY OF ABSTRACT <input checked="" type="checkbox"/> UNCLASSIFIED/UNLIMITED <input type="checkbox"/> SAME AS RPT. <input type="checkbox"/> DTIC USERS		21. ABSTRACT SECURITY CLASSIFICATION UNCLASSIFIED	
22a. NAME OF RESPONSIBLE INDIVIDUAL Dr. Edmond Murad		22b. TELEPHONE (Include Area Code) (617) 377-3176	22c. OFFICE SYMBOL PHK

TABLE OF CONTENTS

<u>Section</u>	<u>Page</u>
1. INTRODUCTION . . . . .	1
2. ANALYSIS . . . . .	2
3. SUMMARY . . . . .	6

Accession For	
NTIS GRA&I	<input checked="" type="checkbox"/>
DTIC TAB	<input type="checkbox"/>
Unannounced	<input type="checkbox"/>
Justification	
By _____	
Distribution/	
Availability Codes	
Dist	Avail and/or Special
<b>A-1</b>	



## 1. INTRODUCTION

This report investigates the feasibility of using advanced focal plane arrays coupled with telescopes as thermal imaging systems for orbiting targets. The infrared signature of a target will depend on a host of intercoupled factors including (1) surface properties (temperature, emissivity, reflectivity), (2) illumination conditions (solar position, earth background temperature), (3) target orientation, location, and dynamics with respect to the observer, and (4) atmospheric conditions along the illumination and target-observer paths. The determination of absolute surface temperatures of an unknown target is certainly a difficult if not infeasible problem without detailed knowledge of all of these factors. Here, we address the somewhat simpler problem of calculating the change in detected signal observed as a function of relative surface temperature differences, or conversely, given a sensor and its inherent characteristics, we attempt to determine the minimum detectable temperature difference measurable for a target surface of known characteristics.

## 2. ANALYSIS

The base case considered is for a 1 meter square planar target with a uniform surface emissivity of 0.85. The surface reflectivity is purely diffuse, i.e., it has no specular component. The target has a temperature of 220 K, and is located directly above the observer, outside of the earth's atmosphere. The observer altitude is 3 km. In addition, four cases similar to this base case (denoted case "A"), but each with one fundamental difference from the base case, were considered:

- (B) The target direct  $\theta$  was  $90^\circ$  from the observer zenith angle, resulting in a long slant path from the observer to the target.
- (C) The target surface emissivity was 0.15 rather than 0.85, changing the relative magnitudes of the target signature components (thermal emission and scattered earthshine).
- (D) The target base temperature was 290 K rather than 220 K.

Target signatures were calculated with the Spectral Sciences Target IR Signature (SSTIRS) code using the  $5 \text{ cm}^{-1}$  LOWTRAN-5 option. Transmitted spectral radiances for cases A-D are plotted in Figures 1-4, respectively. In addition, the earthshine scattering and thermal emission components of the total signatures are also shown in the figures. In case A, these components are comparable in magnitude above  $5 \mu\text{m}$ , but earthshine scattering dominates the signature below  $5 \mu\text{m}$ . Atmospheric absorption by  $\text{H}_2\text{O}$ ,  $\text{CO}_2$ , and  $\text{O}_3$  are apparent in the spectrum. These absorptions are greatly enhanced in case B (see Figure 2), where the observer line-of-sight (LOS) travels along a long slant path to the target. In case C, the surface reflectivity has been enhanced at the expense of the emissivity, and as a result, the intensity of the reflected earthshine dominates the thermal emission (see Figure 3). By increasing the target temperature from 220 K to 290 K, thermal emission is the dominant feature of the target signature (see Figure 4).

For the temperatures considered here (200-300 K), the ideal thermal imaging system would have appreciable sensitivity in the 8-10  $\mu\text{m}$  region to take advantage of the atmospheric transmission window between the 6.3  $\mu\text{m}$

H<sub>2</sub>O and 9.6 μm O<sub>3</sub> absorption bands, and the fact that the peak of the Planck function is near this region at these temperatures. The advanced IrSi focal plane arrays currently under development are potential candidates for such a system. In contrast to PtSi arrays, whose spectral response cuts off at about 6 μm, the theoretical response of an IrSi array extends to almost 12 μm. To date, IrSi focal plane arrays have been built with appreciable response out to 9 μm. The spectral responses of IrSi and PtSi arrays are plotted in Figure 5.

Table 1 contains predictions of the current that would be measured by the advanced IrSi array of Figure 5 in three spectral band passes (assuming a flat filter transmission) in which there is significant atmospheric transmission. The predicted current I is calculated by the equation

$$I = \delta\Omega \int_{\lambda_1}^{\lambda_2} R(\lambda) S(\lambda) d\lambda \quad (1)$$

where  $\delta\Omega$  is the solid angle viewed by a single pixel,  $R(\lambda)$  is the target radiance, and  $S(\lambda)$  is the detector spectral response function.  $\delta\Omega$  was calculated assuming an image scale of 8.25 arcseconds/mm (i.e., the image scale of the AMOS 1.6 m telescope at the Cassegrain focus), and an array diagonal dimension of 20 mm. The spectral band passes chosen, 3.0-4.2, 4.5-5.5, and 8.0-9.5 μm, correspond to the most useful band passes for thermal imagers based on PtSi arrays, current IrSi arrays, and advanced IrSi arrays, respectively. The response of the advanced IrSi array is similar to that of the current IrSi array in the 4.5-5.5 μm region, and similar to that of the PtSi array in the 3.0-4.2 μm region. The following trends can be discerned from Table 1. For the four cases considered here, the most intense signals are associated with case D, because its 290 K temperature yields more thermal radiation. Though the target temperature is only 220 K in case G, its signature is almost as bright as that of case D due to its lower surface emissivity ( $\epsilon=0.15$  for case G vs. 0.85 for the other cases) and resulting higher earthshine reflections. The lowest overall signal is associated with the long slant path case, case B. Comparison of the current predictions for cases A and B show that of the three band passes considered, the 8.0-9.5 μm band pass is least affected by atmospheric attenuation.

The signature calculations for cases A-D were repeated at temperatures 1, 2, 5, and 10 degrees higher than the base temperature for each case. Figures 6-9 plot for cases A-D, respectively, the increase in the current measured by a single pixel of an advanced IrSi array resulting from these temperature increases as calculated by

$$\Delta I(\lambda) = [R(\lambda, T) - R(\lambda, T_0)] S(\lambda) \Delta T \quad (2)$$

where T is the target temperature,  $T_0$  is the base temperature for the case, and the remaining variables have been defined previously. Figures 10-13 plot integrated in-band current as a function of temperature difference for cases A-D, respectively.

In order for a thermal imager to detect a temperature difference, the measured current difference corresponding to the change must be greater than detector current noise levels, and greater than the difference in dark current between adjacent pixels. We have not been able to determine what current noise levels are, or how well the dark current is controlled from pixel to pixel, but the overall sum of these factors is likely less than the magnitude of the dark current itself. The dark current is very strongly dependent on the focal plane array (FPA) temperature. Dark current density for three arrays is plotted as a function of FPA temperature in Figure 14. A pixel diameter of 25  $\mu\text{m}$  has been assumed.

Figures 10-13 can be used to determine temperature sensitivity for any minimum current level criteria. As an example, assume that a temperature difference must induce a detected current change at least as large as dark current levels to be detectable. Then, for a PtSi array at 77 K, the dark current density is about  $8 \times 10^{-15}$  A. Assuming that the pixel resolution at the target is  $1 \text{ m}^2$ , we see in Figure 10 that a PtSi array could not detect a temperature change of 10 K ( $\Delta I$  is about  $2 \times 10^{-15}$  A in the 3.0-4.2  $\mu\text{m}$  band pass for a  $10^\circ$  change). In comparison, the dark current density for an advanced IrSi array at 35 K is about the same as for the 77 K PtSi array, and for the 8.0-9.5  $\mu\text{m}$  band pass, the minimum detectable temperature change is less than  $2^\circ$ .

If imager data is digitized, sensor dynamic range can have significant impact on temperature sensitivity. In this case, the minimum detectable

temperature difference can also be limited by the current associated with one digital bit of dynamic range. For example, for a sensor system with 8 bits of dynamic range, the increase in signal for a given temperature difference must be at least one part in 256 of the total detected signal. When thermal emission dominates the target signature, the signal change for a 1 degree temperature increase for the base temperatures considered here is on the order of a few per cent (compare Table 1 and Figure 10 for case A), and digitization does not significantly limit temperature difference discrimination. In contrast, the signature of a reflective surface such as that of case C can be dominated by reflected earthshine, and though the total signature is brighter than case A, a one degree temperature change is overwhelmed by the total signal (the current difference is less than one part in a thousand of the total signal) and does not trigger a single bit out of 8 regardless of dark current levels.

### 3. SUMMARY

To summarize, the determination of absolute target temperatures is difficult without detailed knowledge of target surface properties and the viewing scenario. The ability of a telescope system to discern temperature differences on a target would be greatly enhanced by the use of advanced IrSi focal plane arrays, due to increased response of these materials in the 8-9  $\mu\text{m}$  atmospheric window region. The minimum detectable temperature difference is ultimately determined by the current noise and pixel-to-pixel current variation of the array, which in turn is very strongly dependent on the focal plane temperature. Dark current densities vary by several orders of magnitude for focal plane temperature differences of only 10 degrees. Therefore, the lower the focal plane temperature can be held, the lower the minimum detectable temperature difference. We have determined the measured current predicted for several viewing scenarios and detector spectral response functions, and have shown that temperature sensitivities on the order of 1 degree are possible for advanced IrSi arrays. Sensor dynamic range can affect temperature sensitivity when images are digitized.

TABLE 1: MEASURED CURRENT PREDICTIONS (A)

BAND PASS (nm)						T(K)	c	TARGET LOCATION
3.0	4.2	4.5	5.5	8.0	9.5			
$2.65 \times 10^{-14}$		$4.44 \times 10^{-14}$		$2.93 \times 10^{-13}$		220	0.85	zenith
$3.29 \times 10^{-15}$		$1.65 \times 10^{-15}$		$4.58 \times 10^{-14}$		220	0.85	slant
$1.41 \times 10^{-13}$		$2.91 \times 10^{-13}$		$9.08 \times 10^{-13}$		220	0.15	zenith
$1.25 \times 10^{-13}$		$2.63 \times 10^{-13}$		$1.01 \times 10^{-12}$		290	0.85	zenith

FIG. 1: 220 K,  $\epsilon = .85$ ,

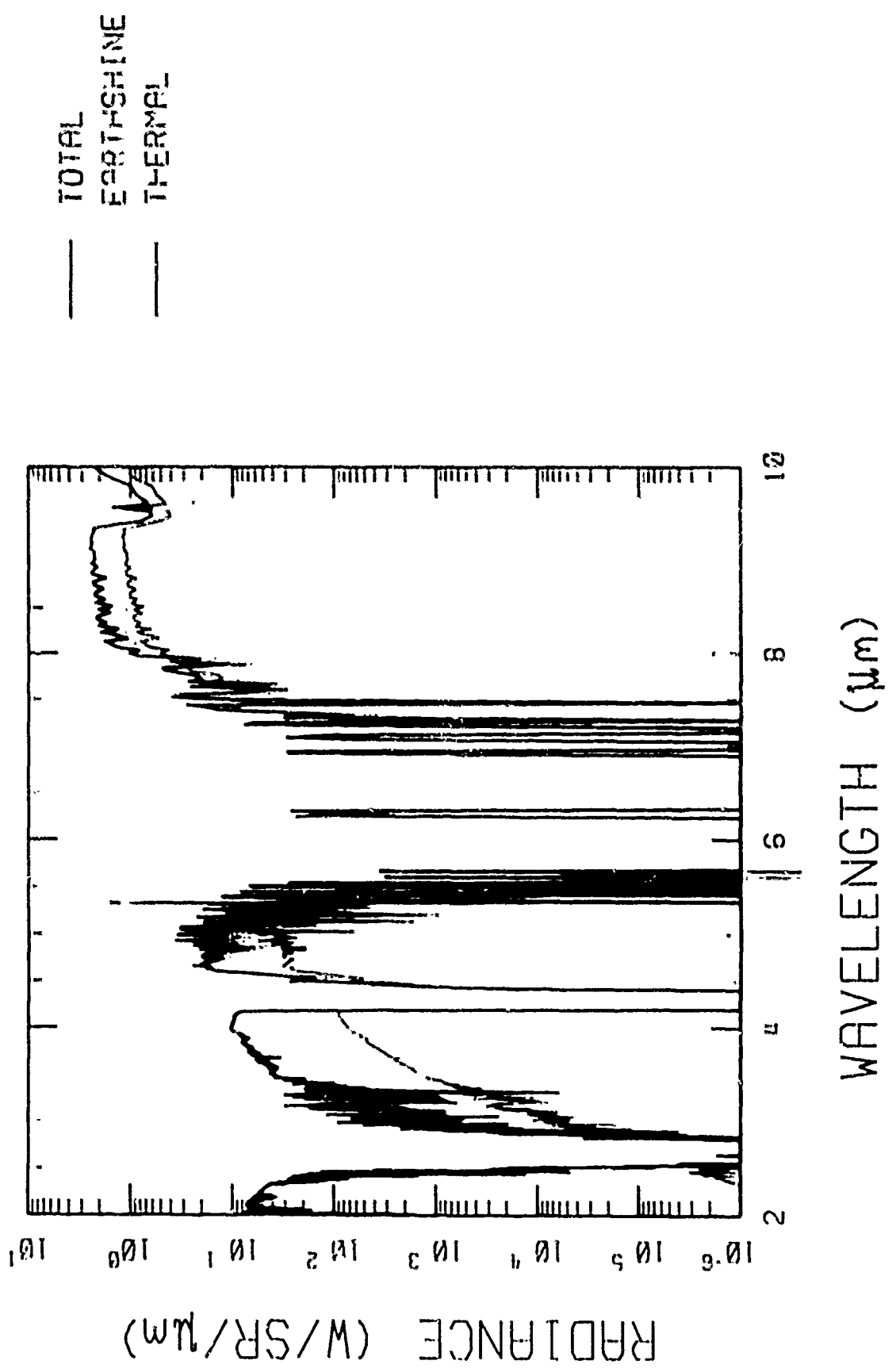


FIG. 1: 220 K,  $\epsilon = .85$ ,

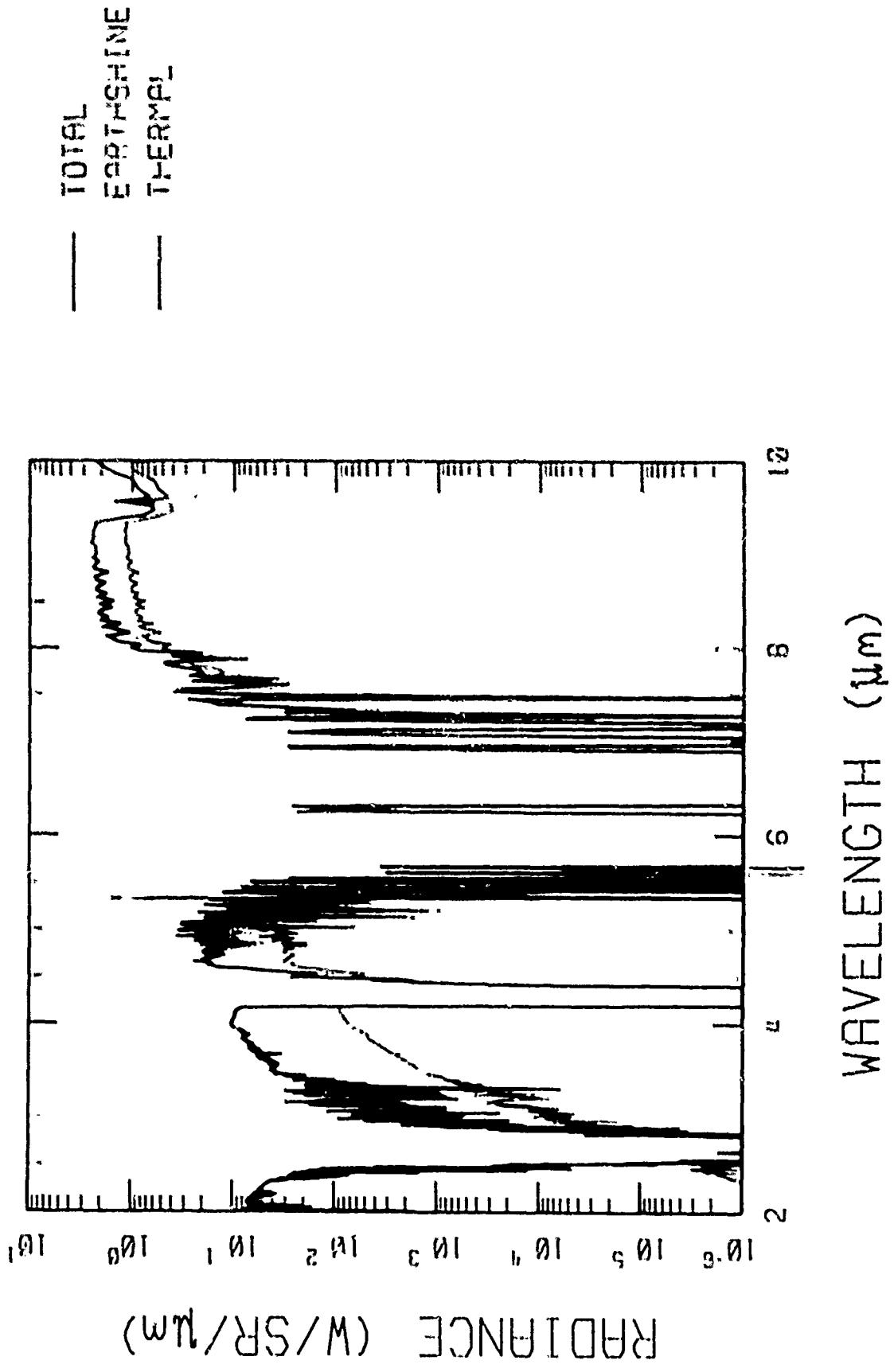


FIG.2: 220 K,  $\epsilon = .85$ , SLANT PATH

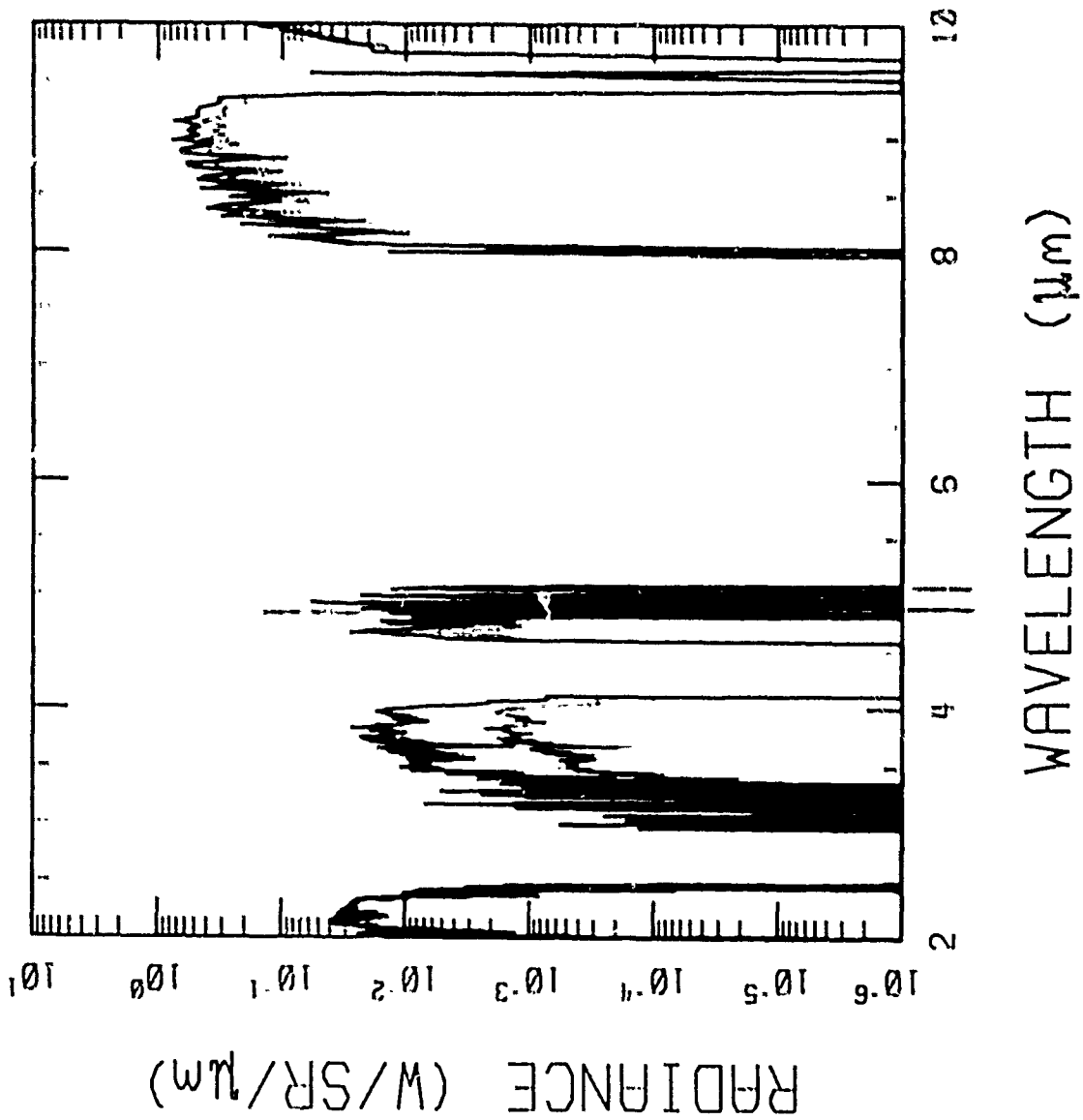


FIG.3: 220 K,  $\epsilon = .15$

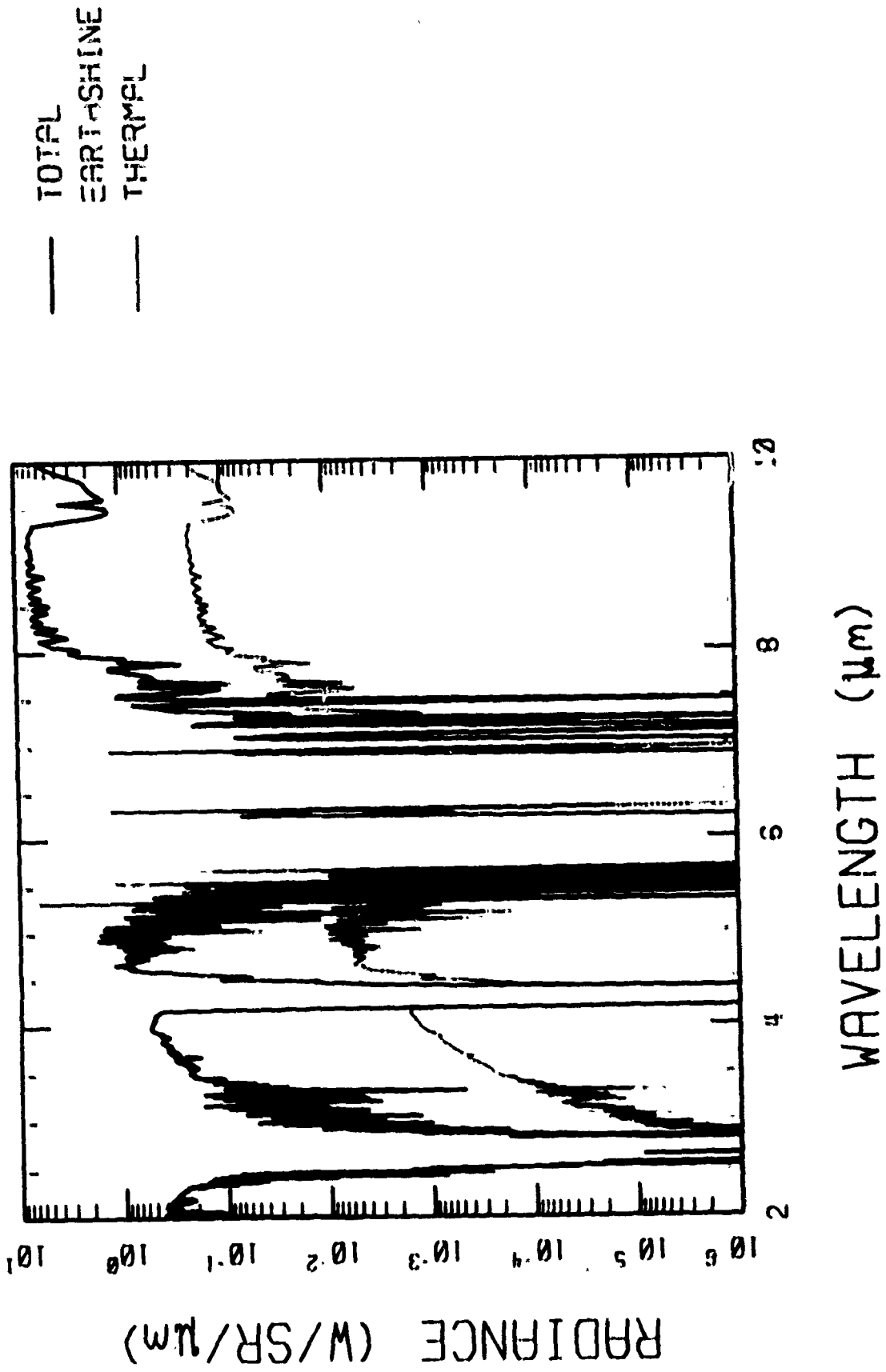


FIG. 4: 290 K,  $\epsilon = 0.85$

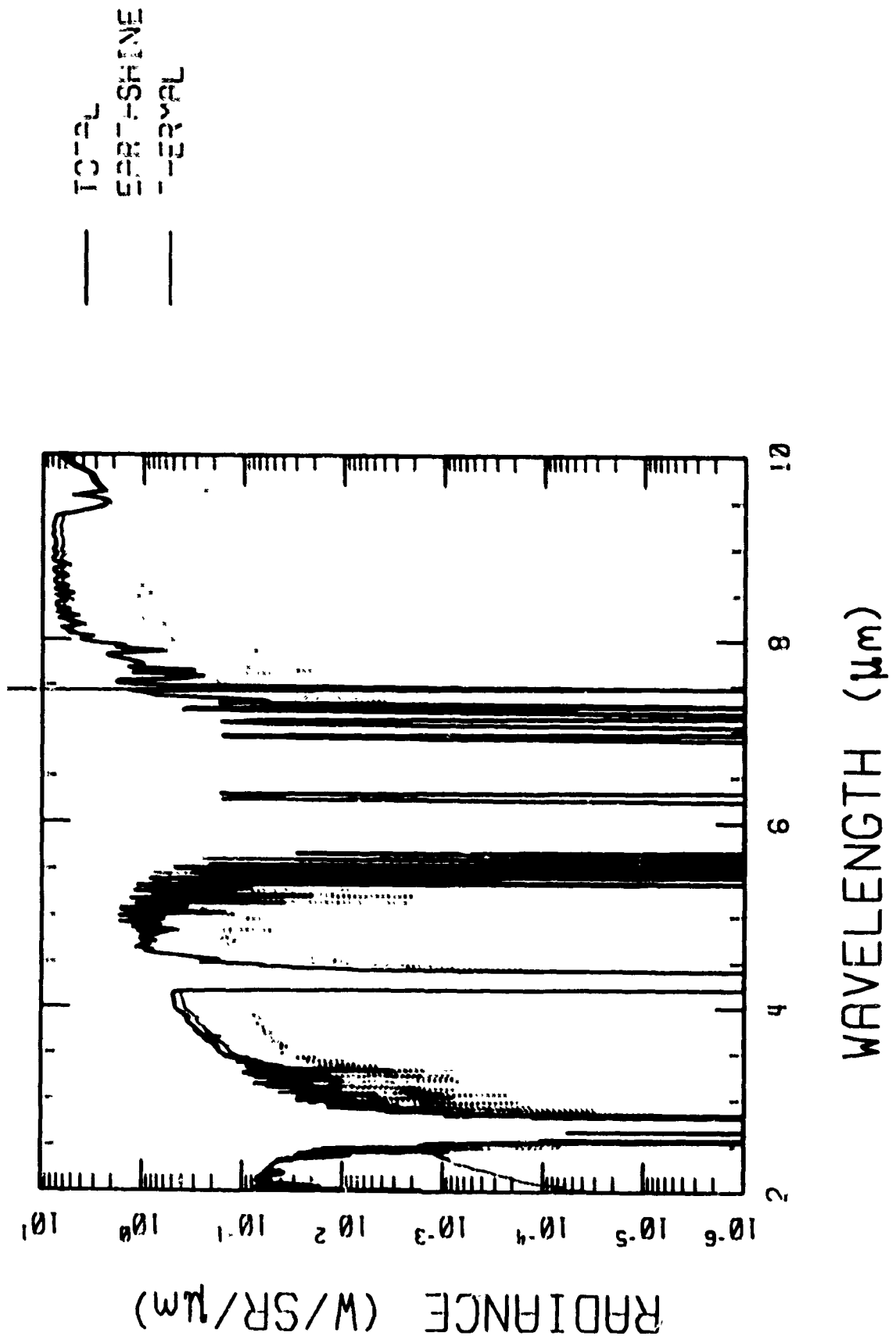


FIG.5: SPECTRAL RESPONSIVITY

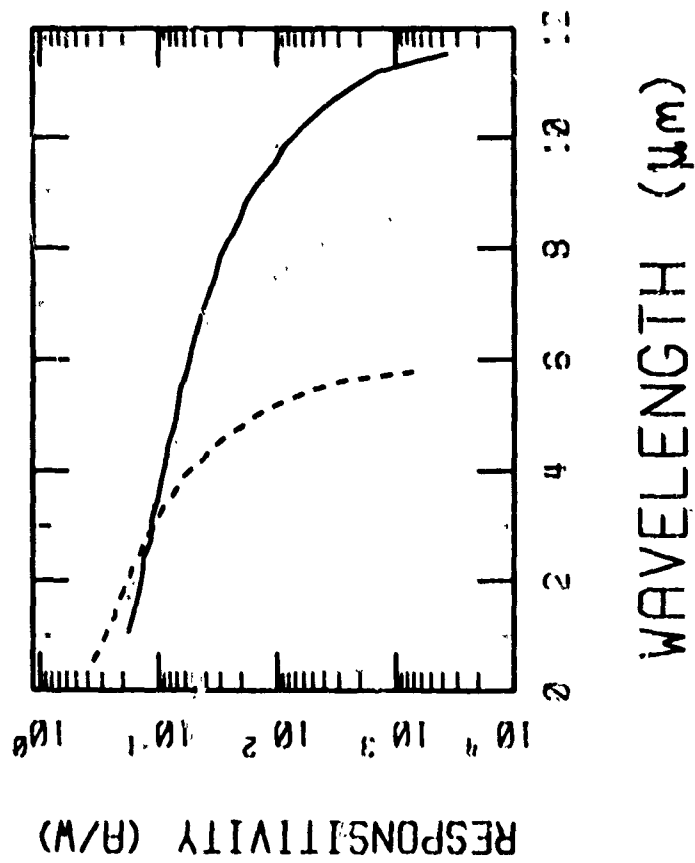


FIG.6: IrSi,  $\epsilon = .85$

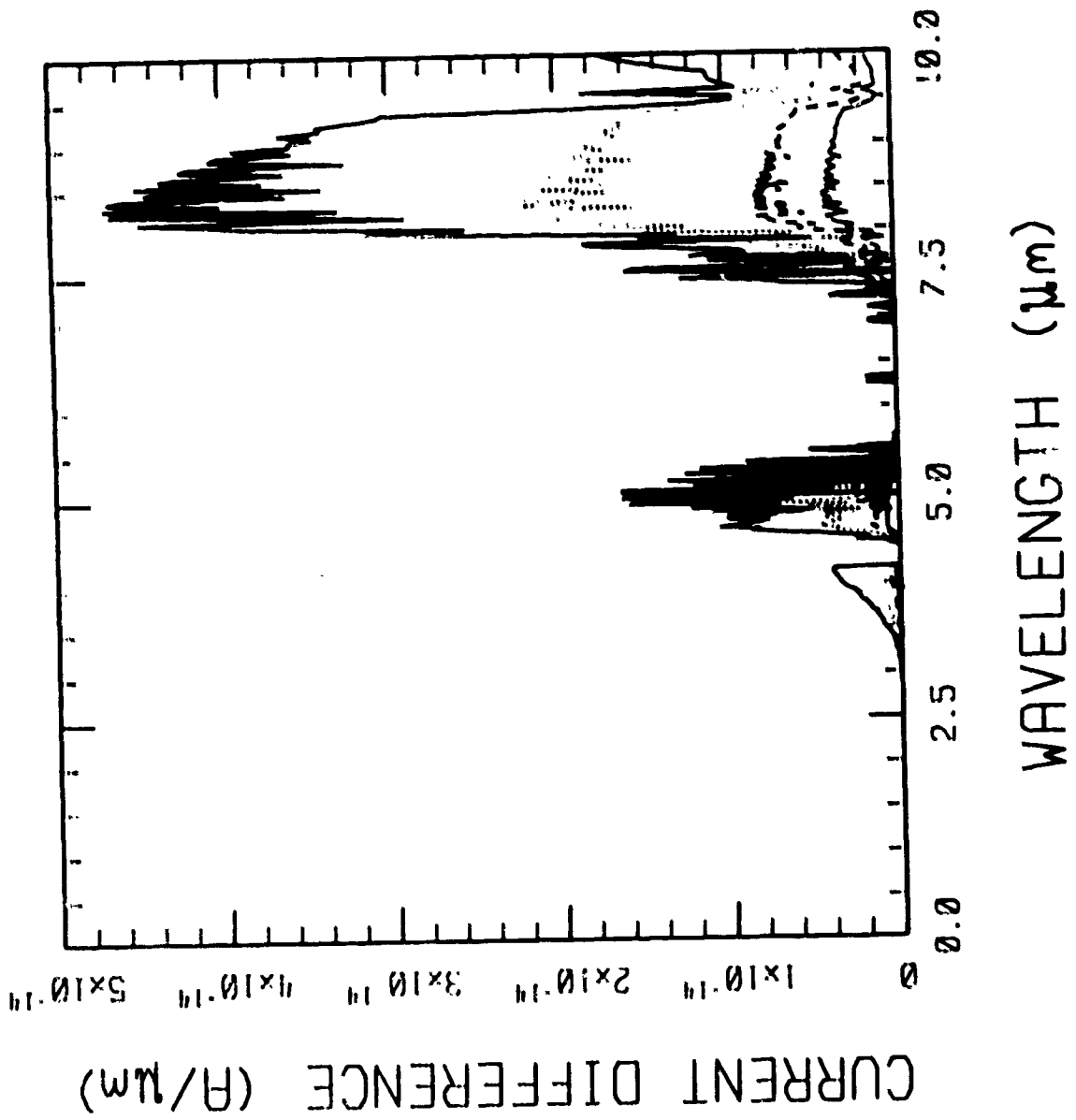


FIG.7: IrSi,  $\epsilon=.85$ , SLANT PATH

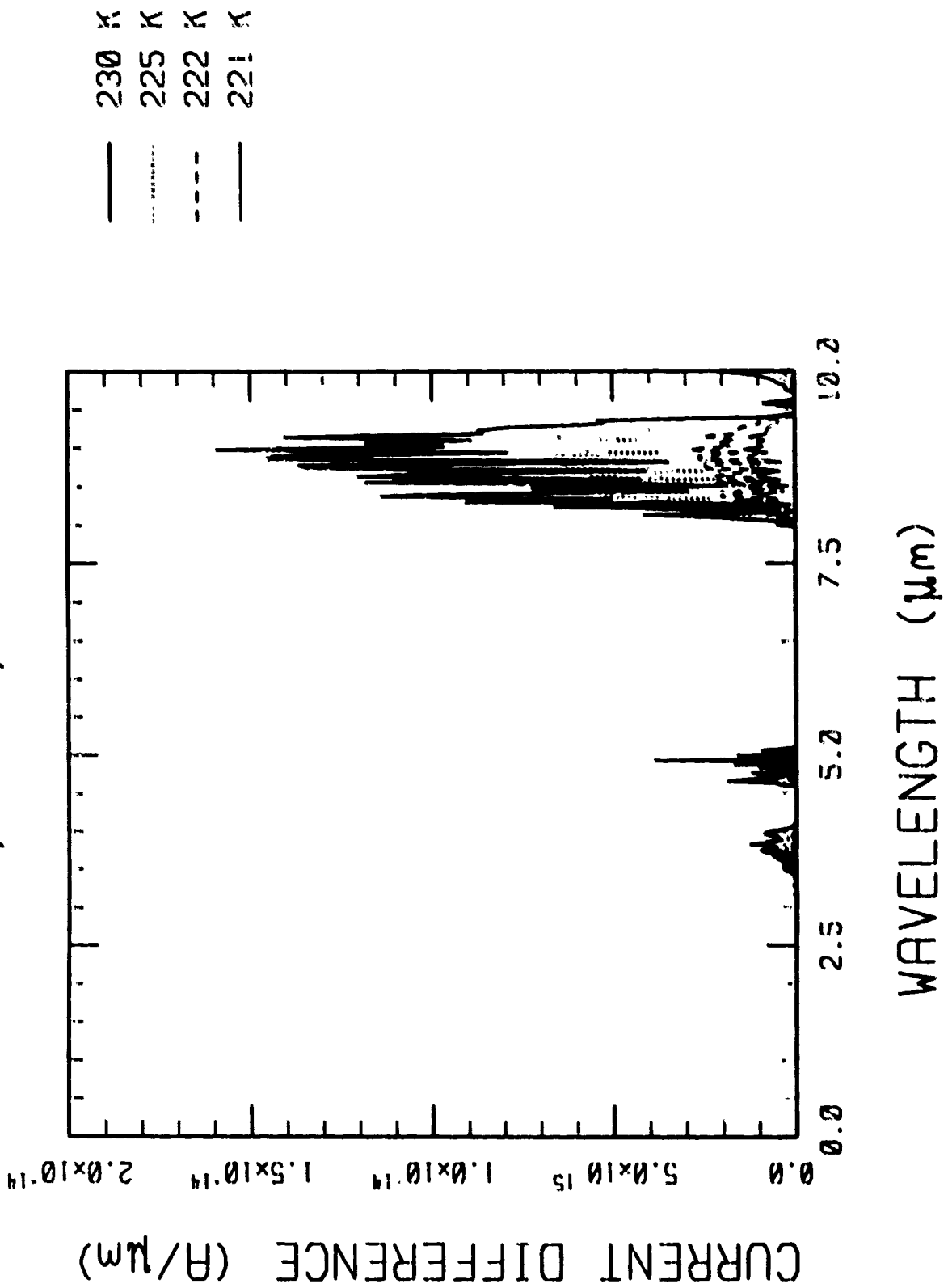


FIG.8: IrSi,  $\epsilon=.15$

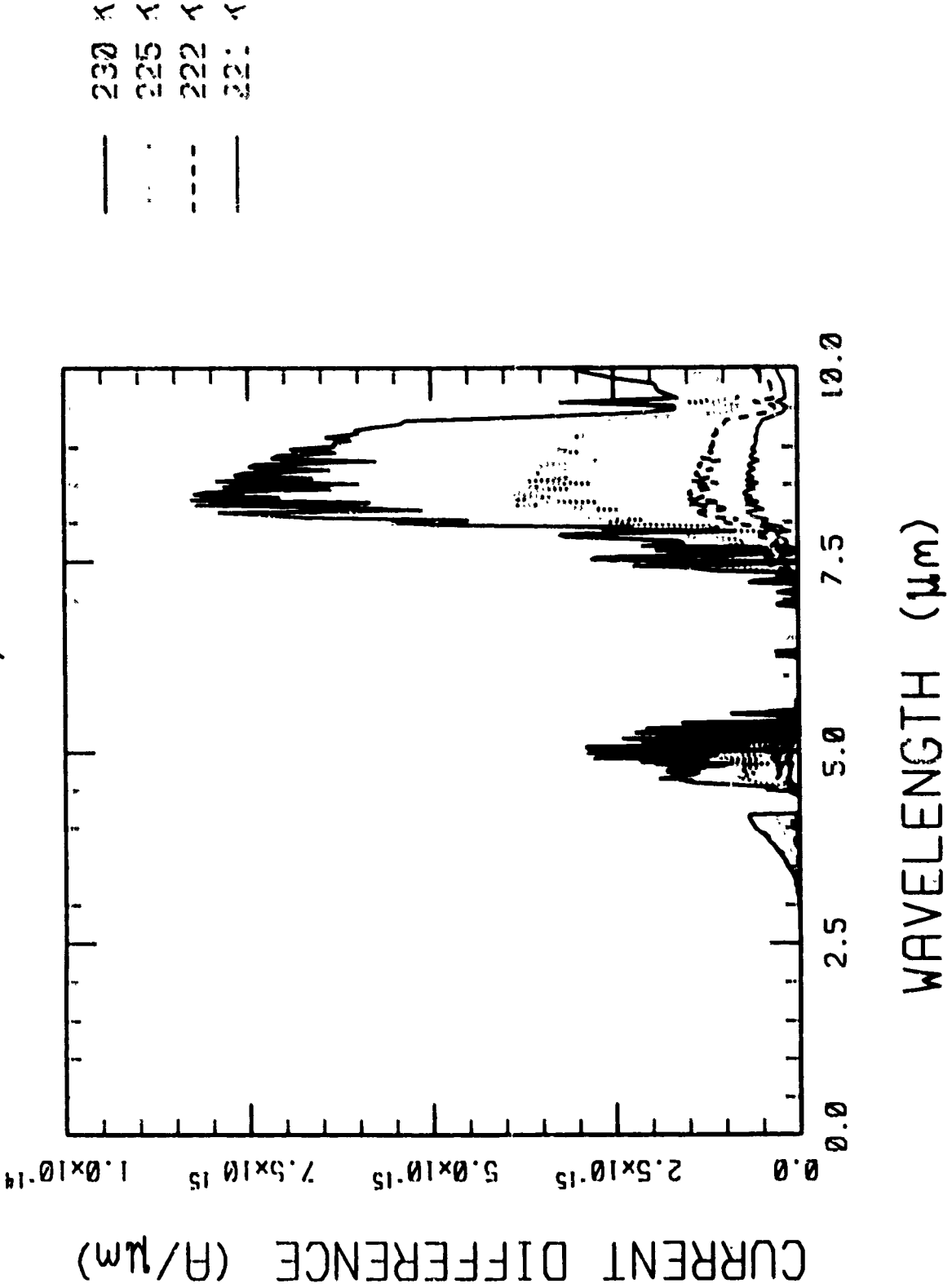


FIG.9: IrSi,  $\epsilon = .85$

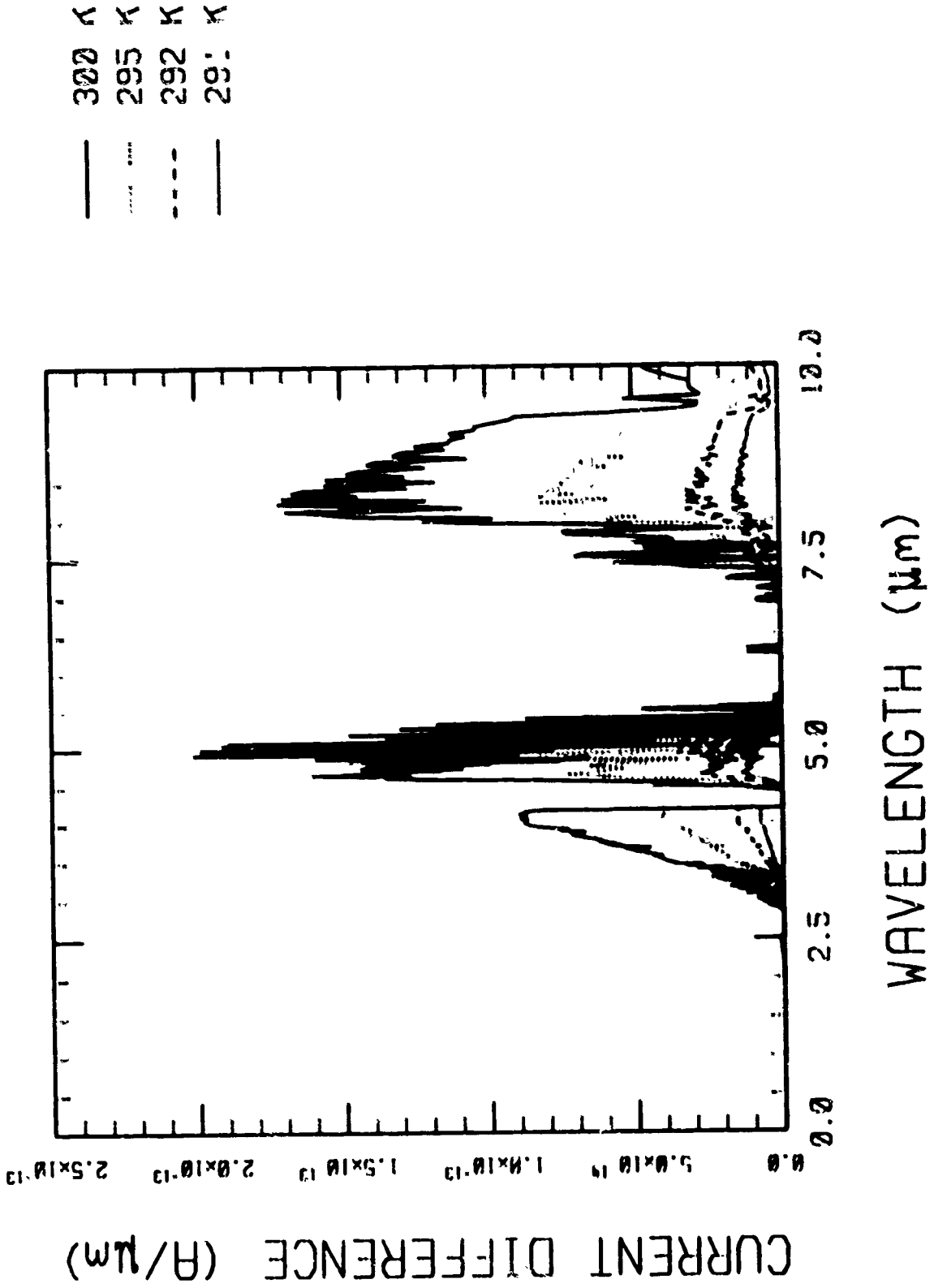


FIG. 10:  $T_0 = 220$  K,  $\epsilon = 0.85$

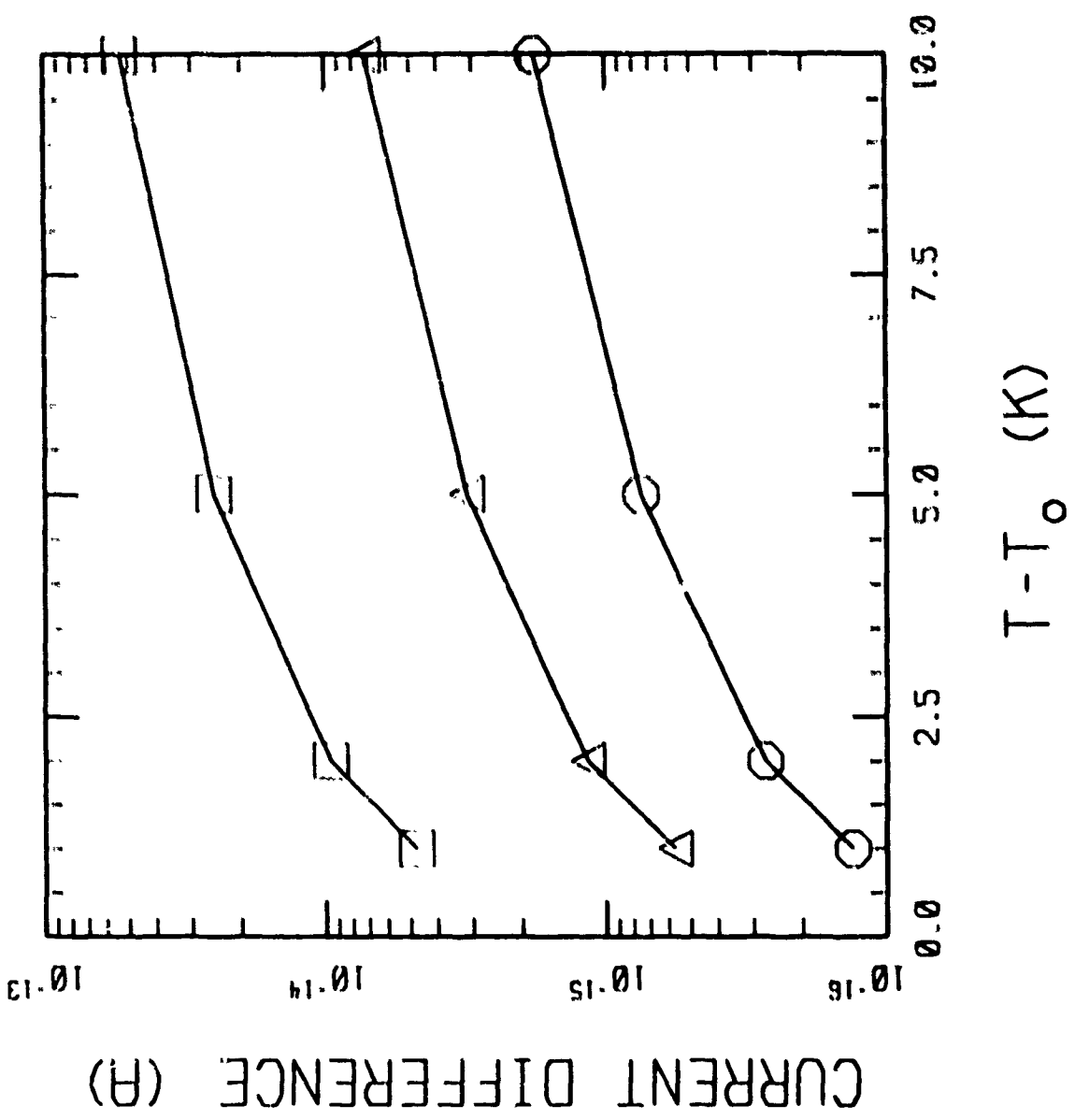


FIG. 11:  $T_0=220$  K,  $\epsilon=0.85$ , SLANT PATH

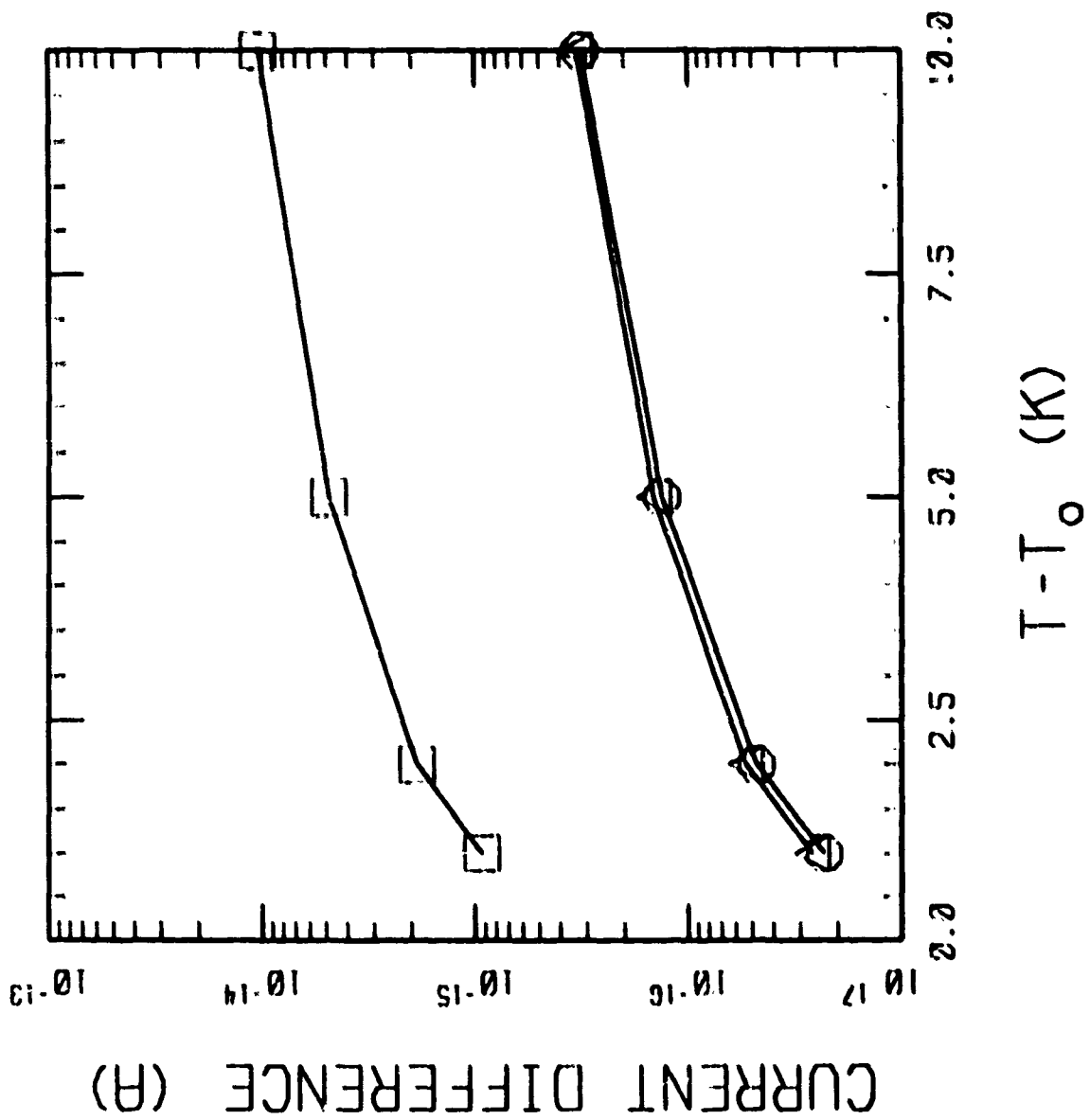


FIG. 12:  $T_0 = 220\text{ K}$ ,  $\epsilon = 0.15$

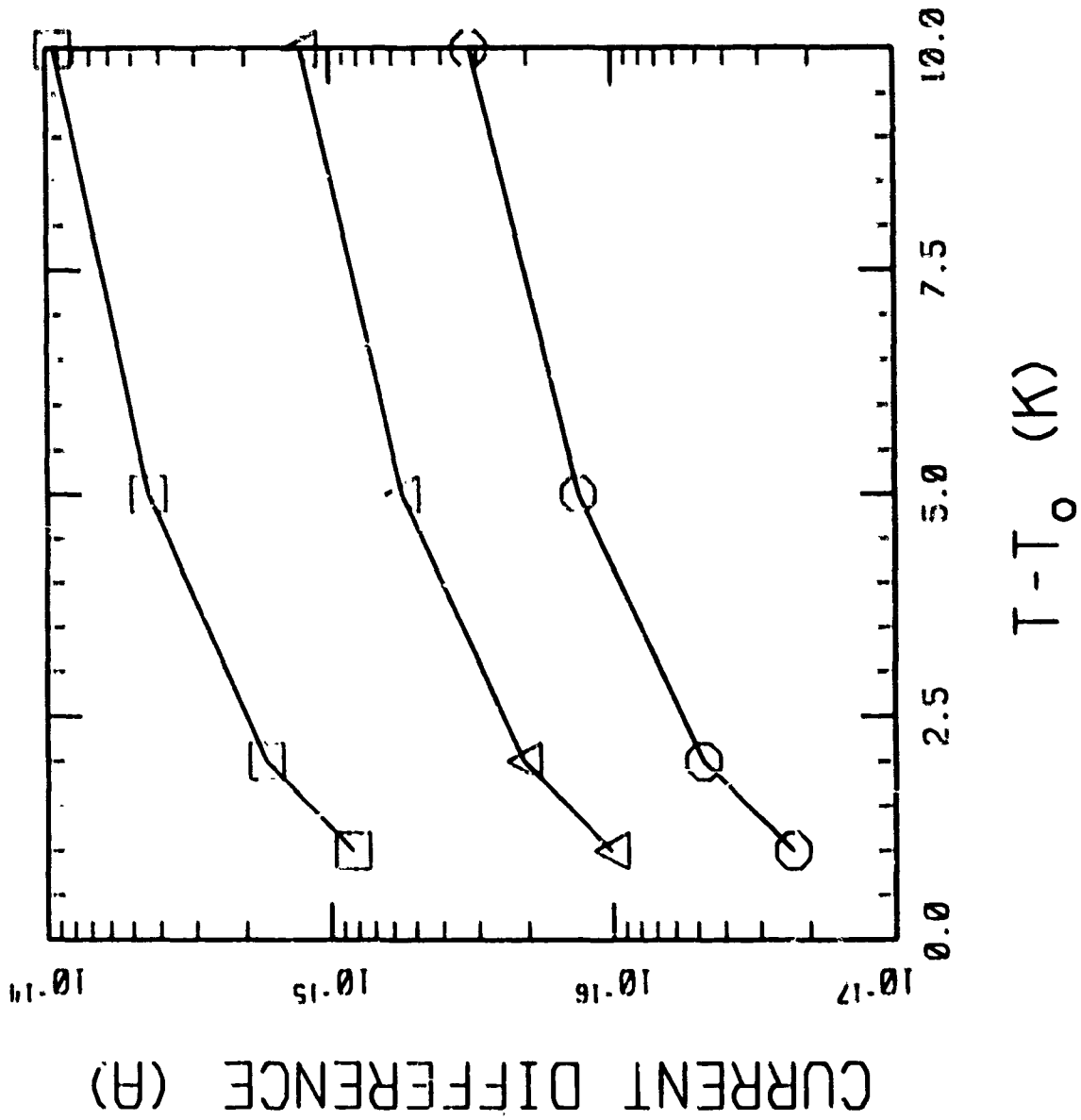


FIG. 13:  $T_0 = 290\text{ K}$ ,  $\epsilon = 0.85$

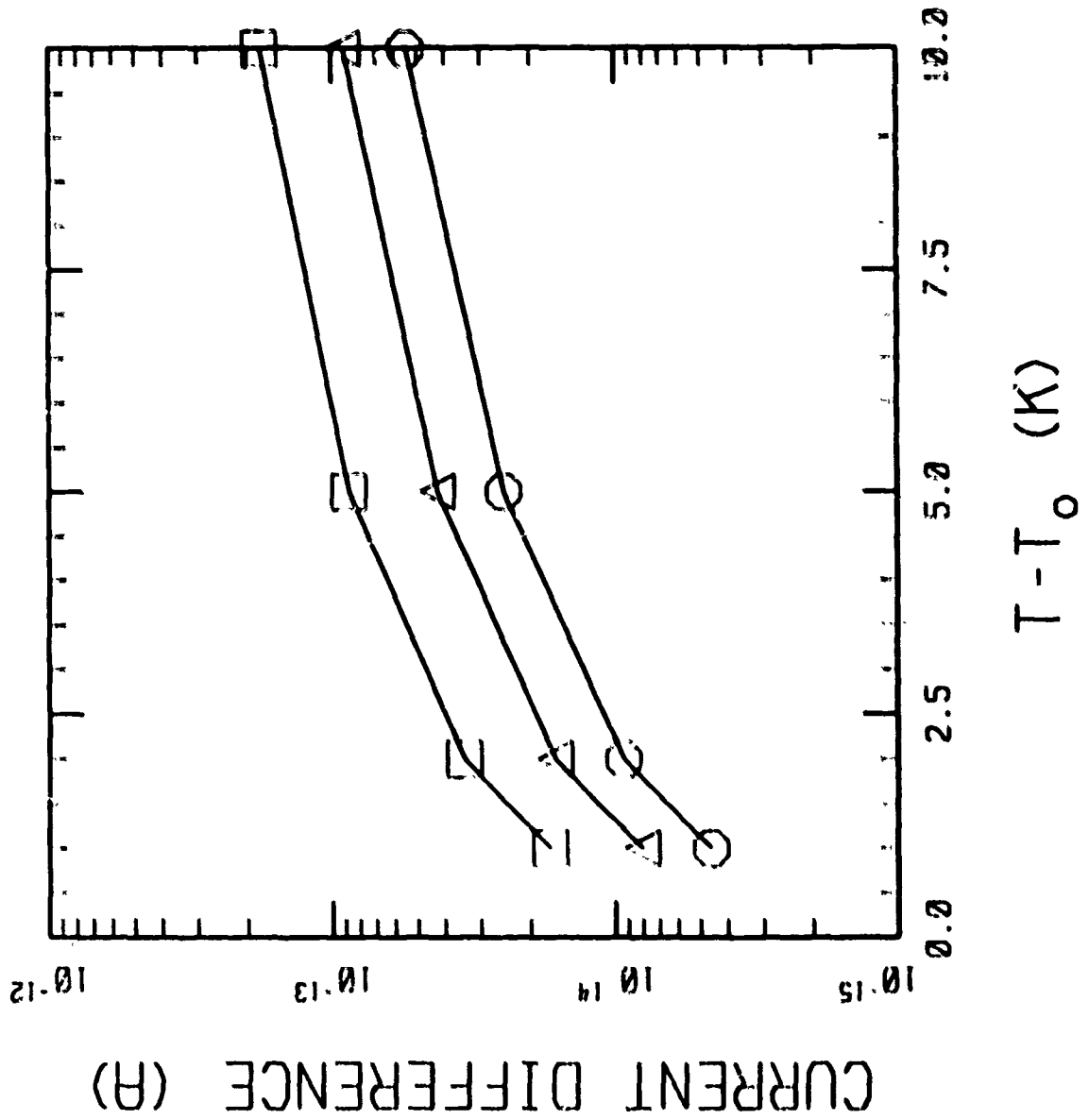


FIG. 14: DARK CURRENT

